Progress in Physics of Applied Materials 3 (2023) 203–209

Semnan University

Progress in Physics of Applied Materials

journal homepage: https://ppam.semnan.ac.ir/

Synthesis of CuO and Ce-doped CuO nanosheets; characterization, optical and magnetic properties

H. Khaleghi

Department of Basic Sciences, Semnan Branch, Islamic Azad University, Semnan, Iran

ARTICLE INFO

Article history:
Received: 26 November 2023
Revised: 20 December 2023
Accepted: 30 December 2023

Keywords:
Ce-doped CuO
Hydrothermal method
Nanosheets
Morphology
Optical and Magnetic Properties
Rare earth element

ABSTRACT

In this article, the structural, magnetic, and optical properties of CuO doped by cerium metal ions as a rare earth element synthesized by the hydrothermal method have been investigated. Various techniques such as X-ray diffraction (XRD) along with Rietveld refinement analysis, energy dispersive X-ray analysis (EDX), and field emission scanning electron microscopy (FESEM) have been used to investigate the crystalline and morphological properties. The results demonstrated that the samples crystallized in the form of polycrystalline and nanosheets with a monoclinic structure. Rietveld refinement of the sample showed sensible accord among the experimental data and standard CuO lattice constants. Also, the existing elements are evenly distributed on the surface of the sample and no impurity elements were observed in the material. By using UV-Vis absorption spectroscopy, the optical band gap of the sample was calculated at an acceptable value. To investigate the magnetic properties, a vibrating sample magnetometer (VSM) was carried out, which showed the weak ferromagnetic property of the Ce-doped sample.

1. Introduction

Today, in addition to various metal nanoparticles, a wide range of metal oxide nanoparticles also play an essential role in various fields, including physics, chemistry, and material science. In the field of technology, metal oxide nanoparticles are widely used in the construction of microelectronic circuits, sensors, fuel cells, and piezoelectric devices [1-6].

CuO is one of the widely used semiconductor oxides, along with MnO_2, SnO_2, and ZnO, which has unique properties and plays a key role in various fields due to its distinct chemical, optical, electronic, and magnetic properties [7-10]. CuO is a p-type metal oxide semiconductor. This nano oxide also has many applications in various fields such as spintronic devices, catalysts, gas sensors, biosensors, photocatalytic degradation, and high-temperature superconductors [11-16]. Doping of CuO nanoparticles with metal ions induces several structural defects in their crystal lattice, such as oxygen vacancies and interstitial defects. These crystal lattice defects can alter the physical and chemical properties of copper oxide, which are important for spintronic device applications and gas sensing properties.

Several researches have been conducted to investigate the effect of transition metals doping such as manganese, cobalt, nickel, iron, lead, and silver, and rare earths such as Y, Ce, Pr, Nd, Sm, Eu, and Tb in the structure of copper oxide on its structural, optical and magnetic properties [17-20].

In research by Gvozdenko et al., it has been shown that CuO nanoparticles combined with gelatin have a high potential for use in food packaging [21, 22]. CuO nanoparticles prepared by the green method are also used to determine the amount of folic acid in food samples [23], detection of phenolic compounds and a pesticide [24], and food packaging applications [25]. CuO nanoparticles used in photovoltaic devices, biosensors, and catalysts in the photodegradation of dyes require some unique properties, which are caused by changing the synthesis process, pH, and doping of different metals [26-28].

* Corresponding author.
E-mail address: hakh1355@yahoo.com

Cite this article as:
Khaleghi, H., 2023. Synthesis of CuO and Ce-doped CuO nanosheets; characterization, optical and magnetic properties. *Progress in Physics of Applied Materials*, *3*(2), pp. 203-209 DOI: **10.22075/PPAM.2023.32447.1071**

In the research article by Gopalakrishnan and Ashokkumar, pure CuO nanoparticles and CuO doped with Ce and Nd rare earth metals was synthesized by the co-precipitation method. The X-ray diffraction pattern of the synthesized nanoparticles showed a monoclinic structure. The secondary phase in the samples was detected as CeO_2 and Nd_2O_3 in the XRD pattern of nanoparticles. According to the FESEM images of the prepared nanoparticles, the mixture of nanorods and nanosheets of CuO nanoparticles became a denser structure when Ce enters the copper oxide lattice. Also, CuO nanoparticles doped with Nd showed a pseudo-sponge structure. FESEM images showed that the synthesized nanoparticles are in the nanoscale range. By UV-Vis spectroscopy, the optical gap for CuO, Ce-doped CuO, and Nd-doped CuO nanoparticles were obtained as 3.6, 3.7, and 3.74 eV, respectively. Due to the doping of CuO by rare earth ions, the Carrier concentration increased, and transferring the Fermi level to the conduction band, led to an increase in the optical gap due to the Burstein-Moss effect. In this study, the antibacterial activity of the synthesized nanoparticles against E. aerogenes bacteria as Gram-negative and B. subtilis as Gram-positive bacteria was investigated [29].

In the research work by Abhilasha et al., pure CuO and Ce-doped CuO nanoparticles were prepared at pHs of 10 and 12 by a one-step co-precipitation method, and the result of pH and Ce concentration on the structural and optical properties of CuO was investigated. XRD analysis of CuO nanoparticles demonstrated its crystalline nature and monoclinic structure. The crystal size obtained from Scherer's equation for pure CuO nanoparticles at pH 10 was about 21.04 nm, which decreased to 15.14 nm with 5% Ce doping. Fingerprint region of the FT-IR spectrum confirmed the formation of CuO nanoparticles and the absorption bands at 852 and 1650 cm^{-1} confirmed the presence of CeO_2 in the monoclinic phase. By measuring the UV-Vis absorption spectrum of pure and Ce-doped CuO nanoparticles, the optical gap of the samples was determined and it was observed that its size depends on the pH value and also the Ce concentration [30].

Various physical and chemical synthesis methods such as sol-gel, hydrothermal, sonochemical, green synthesis, combustion, flux recombination, microwave, and thermal decomposition have been reported in various articles to prepare pure and doped CuO nanostructures with different metals [31-34]. Hydrothermal is one of the common synthesis methods to prepare CuO nanoparticles due to its simple and economical process.

In all review articles and other studies in this area, there are important differences from current research work. These differences include: the synthesis method [35, 36], the physical properties studied [35, 37, 38], the type of precursors [38], the composite or doping [39], the morphology of the nanostructures [35-38], etc. The innovation in the current research paper is that the effect of Ce rare earth metal doping on the structural, optical, and magnetic properties of CuO synthesized with nitrate precursors and by hydrothermal method has been investigated. According to our knowledge, no research has independently investigated the structural, optical, and magnetic properties of Ce-doped CuO with this synthesis method and with these precursors. However, an exhaustive and advanced study of the physical and chemical properties of CuO nanoparticles and their doped samples is still needed. This article provides a detailed analysis of Ce-doping on some physical properties of CuO nanoparticles.

2. Experimental

2.1. Preparation

To provide CuO and $Cu_{0.92}Ce_{0.08}O$ (with abbreviation C.Ce8O) by hydrothermal method, a stoichiometric amount of $Cu(NO_3)_2.3H_2O$ was selected. $Ce(NO_3)_3.6H_2O$ was bought from Central Drag House (P) Ltd. Figure 1 summarizes all the steps of the procedure in a block diagram.

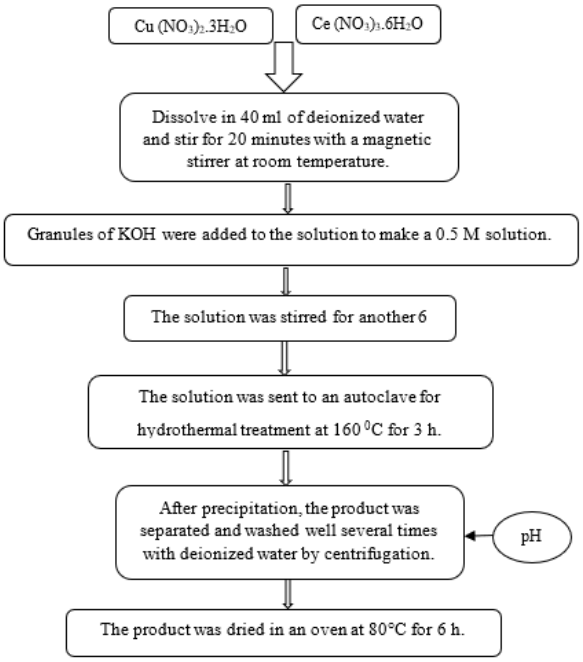

Fig.1. Diagram of the preparation of CuO and C.Ce8O by the hydrothermal method.

2.2. Characterization

The structural properties of CuO and C.Ce8O were analyzed by XRD analysis with an X'pert diffractometer with Cu K_α radiation (λ = 0.15406 nm). The morphological characteristics of the samples were investigated using FESEM (Zeiss Sigma 300HV). Further, EDX analysis was used to determine the compositional proportions.

Optical absorption and band gap energy (E_g) were obtained by UV-Visible spectroscopy of the sample in the wavelength range from 200 to 1100 nm.

VSM in a range of magnetic fields of ±20 kOe was performed using the Lakeshore 7407 to study the magnetic properties of the sample at room temperature.

3. Results and discussion

3.1. Structural properties (XRD analysis)

The XRD patterns of CuO and C.Ce8O is presented in Figure 2, which confirms that two samples have a C2/c space group monoclinic phase correlate with CuO reference code: 00-048-1548. Therefore, the substitution of Ce in the CuO crystal lattice does not affect the monoclinic structure, and Ce ions easily enter the Cu sites inside the CuO crystal lattice. The XRD pattern of the samples contains two

dominant planes (ī11) and (111). According to the XRD patterns, two samples form a single phase without impurities.

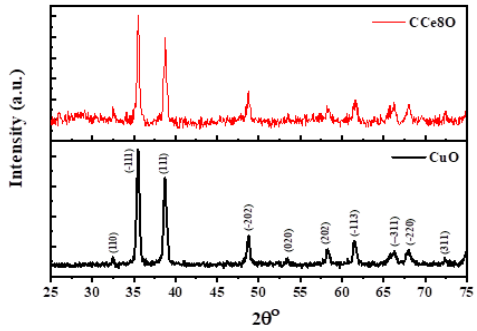

Fig.2. XRD analysis of CuO and C.Ce8O.

The crystallite sizes (D_{sh}) of the two samples are calculated as follows [40]:

$$D_{sh} = k\lambda/(\beta \cos\theta) \quad (1)$$

Where D_{sh}, θ, λ, β, and k are, respectively, the crystallite size, the Bragg diffraction angle, the wavelength of the incident X-ray beam (1.5406 Å), the full width at half maximum (FWHM), and K is a dimensionless shape factor (K = 0.9).

The crystallite size of CuO and C.Ce8O samples were obtained as 57.2 nm and 78.4 nm, respectively.

FullProf software and the Pseudo-Voigt function presented in Figure 3 were utilized to calculate the lattice constants (a, b, and c), β angle, and unit cell volume (V) of C.Ce8O. The parameters obtained by the Rietveld refinement method are a = 4.7132 Å, b = 3.4201 Å, c = 5.1412 Å, β = 99.512°, and V = 81.73Å^3. It can be concluded that the lattice constants, β angle, and V of C.Ce8O correspond to the standard monoclinic parameters of CuO (a = 4.6883 Å, b = 3.4229 Å, c = 5.1319 Å, β = 99.50600, V = 81.22 Å^3). Overall, these results show a good agreement between experimental and theoretical data.

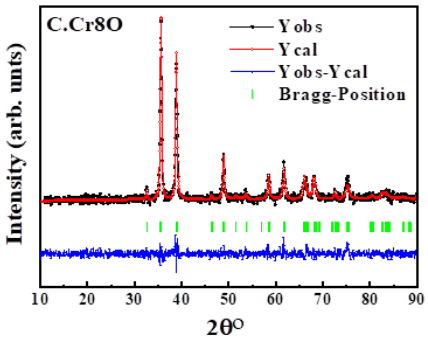

Fig.3. Rietveld refinement of C.Ce8O.

3.2. FESEM and EDX analyzes

The FESEM images of CuO and C.Ce8O nanostructures have been shown in Figure 4. In Figure 4, the nanosheets morphology of the pure CuO is observable. As a result of Ce doping, the morphology of the nanosheets changes significantly and becomes more fragmented.

To study the purity of the elements in the samples, EDX analysis is provided as shown in Figure 5. The results of the EDX analysis are presented in the inset of Figure 5, which shows that the sample is free of additional elements. The existence of extra Au peaks is attributed to the coating of the nanosheet with Au throughout the EDX analysis. The Cu+Ce/O element ratio is about 0.76, which should be exactly 1. The cause for this digression is the entrainment of ambient oxygen during the EDX analysis.

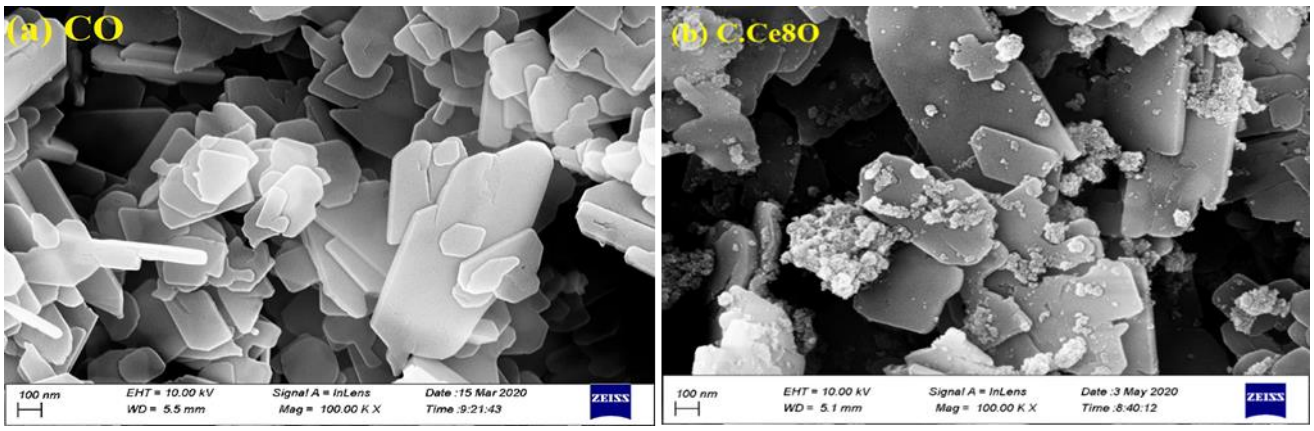

Fig.4. FESEM images of CuO and C.Ce8O.

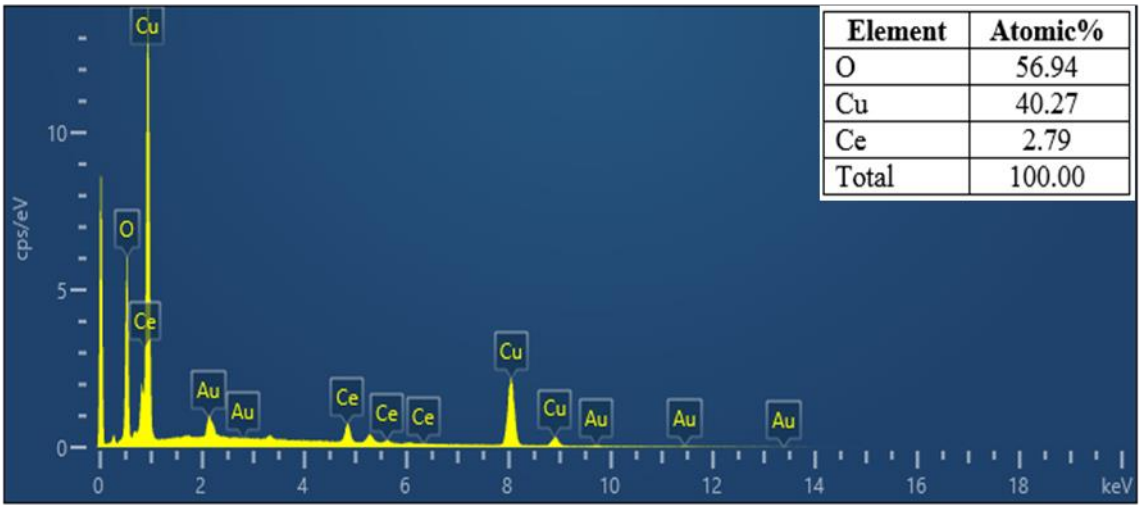

Element	Atomic%
O	56.94
Cu	40.27
Ce	2.79
Total	100.00

Fig.5. EDX spectrums of C.Ce8O.

The Map analysis of the C.Ce8O sample is shown in Figure 6. Characterization of the Map confirmed the monotonous distribution of Cu, Ce, and O on the surface of C.Ce8O. It can be concluded that the above elements are well distributed on the surface of the sample.

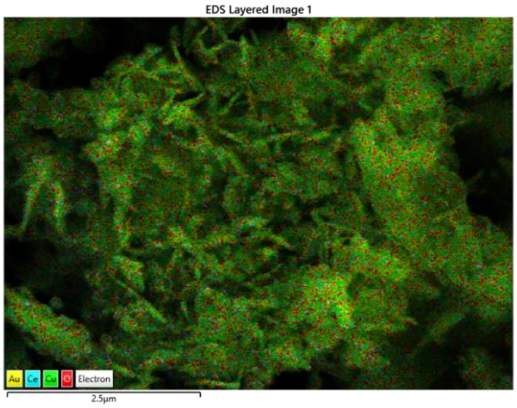

Fig.6. The Map analysis of the C.Ce8O.

3.3. Magnetic properties

Fig.7 shows the M-H curve of C.Ce8O in the magnetic field range of ±20 kOe at room temperature. In several studies, the generic paramagnetic behavior has been reported for pure CuO nanostructures [41, 42]. Considering that cerium ions have a Bohr magneton value, it is expected that a ferromagnetism state will be created when cerium ions enter the crystal structure of copper oxide.

In the study conducted by Theivarasu and Indumathi on pure ZnO and ZnO doped with different concentrations of Ce^{3+}, it was observed that pure zinc oxide has the intrinsic property of diamagnetism, but with the entry of Ce^{3+} ions into the ZnO structure and with increasing concentration of Ce^{3+}, the magnetic state of the sample it gradually has been changed from diamagnetism to ferromagnetism [43].

In the case of sample C.Ce8O, due to the low concentration of Ce^{3+} ions, the state of ferromagnetism is not observed, but it can be expected that with the increase of Ce^{3+} ions in the structure of CuO, the state of paramagnetism will change to ferromagnetism.

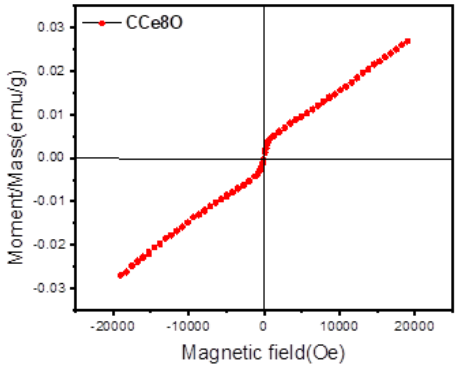

Fig.7. The M-H curves of C.Ce8O at room temperature.

3.4. Optical properties: UV-Vis analyze

To study the optical properties of C.Ce8O, the UV-Vis absorption spectrum of C.Ce8O in the range of 200 to 1100 nm is obtained, as shown in Figure 8. The E_g of the sample can be obtained utilizing the following well-known equation [44]:

$$(\alpha h\nu)^2 = A\,(h\nu - E_g) \qquad (2)$$

Where α, hυ, and A are the absorption coefficient, photon energy, and constant, respectively. The Plot of $(\alpha h\upsilon)^2$ vs. hυ is drawn and presented in the inset of Figure 8. The E_g value was obtained by fitting the data obtained from equation (2) and linearly extrapolating this plot to zero absorbance. The E_g of the sample was equal to 3.68 eV, which is close to the value of 3.7eV reported by Gopalakrishnan and Ashokkumar [29].

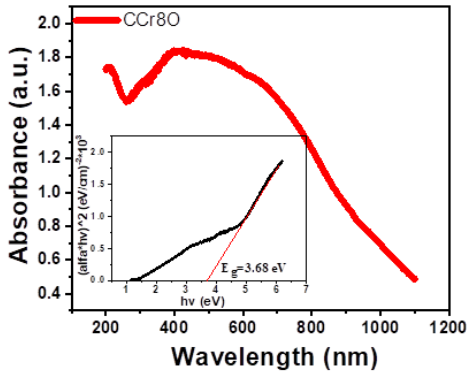

Fig.8. The UV-Vis spectrum of C.Ce8O and Plots of $(\alpha h\upsilon)^2$ vs. hυ.

4. Conclusion

CuO and Cu0.92Ce0.08O samples were prepared by hydrothermal method. XRD analysis determined the crystal phase of samples as monoclinic with a space group C2/c. Lattice constants obtained by the Rietveld refinement method of the doped sample were in good agreement with the data of the standard CuO. FESEM images demonstrated the morphology of nanosheets for pure CuO with variable dimensions, which became somewhat disordered with the introduction of Ce into the crystalline structure of CuO. Further, Map analysis approved the uniform distribution of elements on the surface of the doped sample, and the absence of foreign elements in the sample was proven by EDX analysis.

The VSM hysteresis loop of the doped sample was obtained at room temperature and in the relatively high magnetic field range, which indicated the weak order of ferromagnetism for the doped sample due to the low concentration of the Ce element. As a consequence, changes in the morphological, optical, and magnetic properties of CuO were produced by Ce doping in CuO.

Acknowledgements

There is nothing to acknowledgement.

Conflicts of Interest

The author declares that there is no conflict of interest regarding the publication of this article.

References

[1] Sharma, P.K., Dorlikar, S., Rawat, P., Malik, V., Vats, N., Sharma, M., Rhyee, J.S. and Kaushik, A.K., 2021. Nanotechnology and its application: a review. *Nanotechnology in cancer management*, pp.1-33.

[2] Ahmad, R., Tripathy, N., Ahn, M.S., Bhat, K.S., Mahmoudi, T., Wang, Y., Yoo, J.Y., Kwon, D.W., Yang, H.Y. and Hahn, Y.B., 2017. Highly efficient non-enzymatic glucose sensor based on CuO modified vertically-grown ZnO nanorods on electrode. *Scientific reports*, *7*(1), p.5715. [3] P. Leangtanom *et al.*, "Highly sensitive and selective sensing of H2S gas using precipitation and impregnation-made CuO/SnO2 thick films," *Nanoscale Research Letters,* vol. 16, no. 1, p. 70, 2021.

[4] Cea, P., 2016. The high temperature superconductivity in cuprates: physics of the pseudogap region. *The European Physical Journal B*, *89*, pp.1-54.

[5] Tada, S., Watanabe, F., Kiyota, K., Shimoda, N., Hayashi, R., Takahashi, M., Nariyuki, A., Igarashi, A. and Satokawa, S., 2017. Ag addition to CuO-ZrO2 catalysts promotes methanol synthesis via CO2 hydrogenation. *Journal of Catalysis*, *351*, pp.107-118.

[6] Hao, L., Zhang, Y., Kubomura, R., Ozeki, S., Liu, S., Yoshida, H., Jin, Y. and Lu, Y., 2021. Preparation and thermoelectric properties of CuAlO2 compacts by tape casting followed by SPS. *Journal of Alloys and Compounds*, *853*, p.157086.

[7] Koffyberg, F.P. and Benko, F.A., 1982. A photoelectrochemical determination of the position of the conduction and valence band edges of p-type CuO. *Journal of Applied Physics*, *53*(2), pp.1173-1177.

[8] Mohamed, R.M., Harraz, F.A. and Shawky, A., 2014. CuO nanobelts synthesized by a template-free hydrothermal approach with optical and magnetic characteristics. *Ceramics International*, *40*(1), pp.2127-2133.

[9] Tranquada, J.M., Sternlieb, B.J., Axe, J.D., Nakamura, Y. and Uchida, S.I., 1995. Evidence for stripe correlations of spins and holes in copper oxide superconductors. *nature*, *375*(6532), pp.561-563.

[10] Muhibbullah, M., Hakim, M.O. and Choudhury, M.G.M., 2003. Studies on Seebeck effect in spray deposited CuO thin film on glass substrate. *Thin Solid Films*, *423*(1), pp.103-107.

[11] Gaur, U.K., Kumar, A. and Varma, G.D., 2014. The synthesis of self-assembled polycrystalline 1-D CuO nanostructures in aqueous medium and a study of their multifunctional features. *CrystEngComm*, *16*(14), pp.3005-3014.

[12] Zhang, J., Liu, J., Peng, Q., Wang, X. and Li, Y., 2006. Nearly monodisperse Cu2O and CuO nanospheres: preparation and applications for sensitive gas sensors. *Chemistry of materials*, *18*(4), pp.867-871.

[13] Gou, L. and Murphy, C.J., 2003. Solution-phase synthesis of Cu2O nanocubes. *Nano Letters*, *3*(2), pp.231-234.

[14] Kumar, K. and Chowdhury, A., 2017. Facile synthesis of CuO nanorods obtained without any template and/or surfactant. *Ceramics International*, *43*(16), pp.13943-13947.

[15] Gao, D., Yang, G., Li, J., Zhang, J., Zhang, J. and Xue, D., 2010. Room-temperature ferromagnetism of flowerlike CuO nanostructures. *The Journal of Physical Chemistry C*, *114*(43), pp.18347-18351.

[16] Kafi Ahmadi, L. and Khademinia, S., 2022. Fabrication, characterization, and photocatalytic degradation of malachite green by CuO nanocatalyst. *Progress in Physics of Applied Materials*, *2*(2), pp.83-92.

[17] Basith, N.M., Vijaya, J.J., Kennedy, L.J. and Bououdina, M., 2013. Structural, optical and room-temperature ferromagnetic properties of Fe-doped CuO nanostructures. *Physica E: Low-dimensional Systems and Nanostructures*, *53*, pp.193-199.

[18] Huang, J., Wu, H., Cao, D. and Wang, G., 2012. Influence of Ag doped CuO nanosheet arrays on electrochemical behaviors for supercapacitors. *Electrochimica Acta*, *75*, pp.208-212.

[19] Ponnarasan, V. and Krishnan, A., 2017. Synthesis, structural and optical properties of cobalt doped CuO nanoparticles. *International Journal of Nanoscience*, *16*(02), p.1650031.

[20] Jayaprakash, J., Srinivasan, N., Chandrasekaran, P. and Girija, E.K., 2015. Synthesis and characterization of cluster of grapes like pure and Zinc-doped CuO nanoparticles by sol–gel method. *Spectrochimica Acta Part A: Molecular and Biomolecular Spectroscopy*, *136*, pp.1803-1806.

[21] Gvozdenko, A.A., Siddiqui, S.A., Blinov, A.V., Golik, A.B., Nagdalian, A.A., Maglakelidze, D.G., Statsenko, E.N., Pirogov, M.A., Blinova, A.A., Sizonenko, M.N. and Simonov, A.N., 2022. Synthesis of CuO nanoparticles stabilized with gelatin for potential use in food packaging applications. *Scientific reports*, *12*(1), p.12843.

[22] Blinov, A.V., Gvozdenko, A.A., Yasnaya, M.A., Blinova, A.A., Kravtsov, A.A., Krandievsky, S.O. and Kramarenko, V.N., 2020. Synthesing and studying the structure of nanoscale copper (II) oxide stabilized by polyethylene glycol. *Her Bauman Moscow State Tech. Univ. Ser. Nat. Sci*, *3*, pp.56-70.

[23] Hasan, I.M., Abd-Elsabur, K.M., Assaf, F.H. and Abd-Elsabour, M., 2022. Folic acid determination in food samples using green synthesized copper oxide nanoparticles and electro-poly (methyl orange) sensor. *Electrocatalysis*, *13*(6), pp.759-772.

[24] Pino, F., Mayorga-Martinez, C.C. and Merkoçi, A., 2016. High-performance sensor based on copper oxide nanoparticles for dual detection of phenolic compounds and a pesticide. *Electrochemistry Communications*, *71*, pp.33-37.

[25] Kumar, A., Choudhary, A., Kaur, H., Mehta, S. and Husen, A., 2021. Metal-based nanoparticles, sensors, and their multifaceted application in food packaging. *Journal of Nanobiotechnology*, *19*(1), p.256.

[26] Siddiqui, H., Parra, M.R., Pandey, P., Qureshi, M.S. and Haque, F.Z., 2020. Utility of copper oxide nanoparticles (CuO-NPs) as efficient electron donor material in bulk-heterojunction solar cells with enhanced power conversion efficiency. *Journal of Science: Advanced Materials and Devices*, *5*(1), pp.104-110.

[27] Jayakodi, S. and Shanmugam, V.K., 2020. Green synthesis of CuO nanoparticles and its application on toxicology evaluation. *Biointerface Res. Appl. Chem*, *10*(5), pp.6343-6353.

[28] Thangamani, C., Ponnar, M., Priyadharshini, P., Monisha, P., Gomathi, S.S. and Pushpanathan, K., 2019. Magnetic behavior of ni-doped cuo nanoparticles synthesized by microwave irradiation method. *Surface Review and Letters*, *26*(05), p.1850184.

[29] Gopalakrishnan, R. and Ashokkumar, M., 2021. Rare earth metals (Ce and Nd) induced modifications on structural, morphological, and photoluminescence properties of CuO nanoparticles and antibacterial application. *Journal of Molecular Structure*, *1244*, p.131207.

[30] Abhilasha, Kumari, N. and Gautam, R., 2023. Investigation of impact of pH and rare earth metal dopant concentration on structural, optical and thermal properties of CuO nanoparticles. *Applied Physics A*, *129*(1), p.64.

[31] Rao, M.P., Wu, J.J., Asiri, A.M., Anandan, S. and Ashokkumar, M., 2018. Photocatalytic properties of hierarchical CuO nanosheets synthesized by a solution phase method. *Journal of Environmental Sciences*, *69*, pp.115-124.

[32] Reddy, K.R., 2017. Green synthesis, morphological and optical studies of CuO nanoparticles. *Journal of Molecular Structure*, *1150*, pp.553-557.

[33] Basith, N.M., Vijaya, J.J., Kennedy, L.J. and Bououdina, M., 2014. Structural, morphological, optical, and magnetic properties of Ni-doped CuO nanostructures prepared by a rapid microwave combustion method. *Materials science in semiconductor processing*, *17*, pp.110-118.

[34] Bhattacharjee, A. and Ahmaruzzaman, M., 2018. Microwave assisted facile and green route for synthesis of CuO nanoleaves and their efficacy as a catalyst for reduction and degradation of hazardous organic compounds. *Journal of Photochemistry and Photobiology A: Chemistry*, *353*, pp.215-228.

[35] Islam, M.R., Saiduzzaman, M., Nishat, S.S., Kabir, A. and Farhad, S.F.U., 2021. Synthesis, characterization and visible light-responsive photocatalysis properties of Ce doped CuO nanoparticles: a combined experimental and DFT+ U study. *Colloids and Surfaces A: Physicochemical and Engineering Aspects*, *617*, p.126386.

[36] Velliyan, S. and Rajendran, V., 2021. Study on the effect of Ce3+ doping on structural, morphological and optical properties of CuO nanoparticles synthesized via combustion technique. *Physica B: Condensed Matter*, *613*, p.413015.

[37] Lv, Y., Li, L., Yin, P. and Lei, T., 2020. Synthesis and evaluation of the structural and antibacterial properties of doped copper oxide. *Dalton Transactions*, *49*(15), pp.4699-4709.

[38] Chen, Y., Tan, H., Wu, X., Sun, Q., Wang, D. and Wang, Y., 2019. Effect of doping Ce ions on morphology and photocatalytic activity of CuO nanostructures. *Crystal Research and Technology*, *54*(9), p.1900033.

[39] Bosigo, R., Lepodise, L.M., Kuvarega, A. and Muiva, C., 2021. Hydrothermal synthesis of CuO and CeO2/CuO nanostructures: spectroscopic and temperature dependent electrical properties. *Journal of Materials Science: Materials in Electronics*, *32*(6), pp.7136-7152.

[40] Khaleghi, H. and Ehsani, M.H., 2022. Synthesis and characterization of TM-doped CuO nanosheets (TM= Fe, Mn). *Applied Physics A*, *128*(11), p.969.

[41] Swatsitang, E., Karaphun, A. and Putjuso, T., 2020. Influence of Fe: Co co–doping on the morphology, optical and magnetic properties of Cu1-(x+ y) FexCoyO nanostructures prepared by a hydrothermal method. *Physica B: Condensed Matter*, *583*, p.412044.

[42] Singh, B.P., Chaudhary, M., Kumar, A., Singh, A.K., Gautam, Y.K., Rani, S. and Walia, R., 2020. Effect of Co and Mn doping on the morphological, optical and magnetic properties of CuO nanostructures. *Solid State Sciences*, *106*, p.106296.
[43] Theivarasu, C. and Indumathi, T., 2017. Effect of rare earth metal ion Ce 3+ on the structural, optical and magnetic properties of ZnO nanoparticles synthesized by the co-precipitation method. *Journal of Materials Science: Materials in Electronics*, *28*, pp.3664-3671.
[44] Esmaeili, S., Ehsani, M.H. and Fazli, M., 2020. Photo-catalytic activities of La0. 7Ba 0.3 MnO3 nanoparticles. *Optik*, *216*, p.164812.